A Zeno Paradox: Some Well-known Nonlinear Dopant Drift Memristor Models Have Infinite Resistive Switching Time

Resat MUTLU [1], Tugce Dabanoglu KUMRU [2]

[1] Dept. of Electronics and Communication Engineering, Tekirdağ Namik Kemal University, 59860 Corlu, Tekirdağ, Turkey
[2] Dept. of Research and Development, Hema Industry, 59500 Cerkezkoy, Tekirdag, Turkey

rmutlu@nku.edu.tr, tugcedabanoglu@hattat.com.tr

Submitted December 15, 2022 / Accepted May 14, 2023 / Online first June 2, 2023

Abstract. *There are nonlinear drift memristor models utilizing window functions in the literature. The resistive memories can also be modeled using memristors. If the memristor's resistance switches from its minimum value to its maximum value or from its maximum value to its minimum value, the transition phenomenon is called resistive or memristive switching. The value of the time required for this transition is especially important for resistive computer memory applications. The switching time is measured by experiments and should be calculatable from the parameters of the memristor model used. In the literature, to the best of our knowledge, the resistive switching times have not been calculated except for the HP memristor model and a piecewise linear memristor model. In this study, the memristive switching times of some of the well-known memristor models using a window function are calculated and found to be infinite. This is not feasible according to the experiments in which a finite memristive switching time is reported. Inspired by these results, a new memristor window function that results in a finite switching time is proposed. The results of this study and the criteria given here can be used to make more realistic memristor models in the future.*

Keywords

Memristor, memristor models, nonlinear dopant drift, window function, memristive switching, Zeno paradox

1. Introduction

Dr. Chua defined the memristor as the new and fourth passive circuit element besides the resistor, inductor, and capacitor in his seminal article published in 1971 [1]. An ideal memristor is a passive circuit element with two terminals and a nonlinear relationship between magnetic flux and electrical charge. It has a charge-dependent resistance called memristance and also consumes power [1]. Memristive systems, which are systems with similar properties to memristors, have been introduced in 1976 [2]. Almost four decades later than Dr. Chua's claim, a nano-sized TiO_2 thin film memristive system produced in Hewlett-Packard (HP) laboratory is shown to exhibit the characteristics of a memristor similar to those predicted by Chua during its operation [3], [4]. Thus, the existence of a new nonlinear electronic circuit element, which behaves as if a memristor at least in some part of its operation region, has been announced to the world in 2008 and the memristor and memristive systems have become popular study areas [5–10]. Non-volatile memory and Dynamic Load applications of memristors have been overviewed in [6]. Memory effects are pretty common in nanoscale devices and some of the effects can be modeled using memristors [6]. Resistive memories also behave as memristors [7]. The applications of the memristor in circuit design and computer technology are reviewed in [8]. Memristor usage in memory, analog, logic, and neuromorphic circuit applications is examined in [9]. The discrete and array device applications of memristors have been categorized in [10]. Electronic circuits such as filters, amplifiers [11], oscillators, computer memories [8], and artificial neural network circuits [12] can be listed as examples of the memristor-based circuit application areas. The memristors with substantial threshold voltage values can be used to make amplifiers and filters [13], [14] since a memristor behaves as an LTI resistor under the threshold voltage, and the resistance of a memristor can be tuned to have an adjustable gain or an adjustable cut-off frequency in such circuits [11], [13–15]. Some of the memristor research has focused on modeling the new circuit element. The first and the simplest physical model of a memristor has been presented by HP in [3]. Williams et al. have given the HP memristor model with the assumption that the ion drift speed within the memristor is proportional to the memristor current and homogenous within the memristor. The model is easy to understand however it has linear dopant drift and is obsolete now. Since the homogeneous dispersion of the ions of the model does not match reality, memristor models with nonlinear ion drift speed, which make use of window functions, have been developed to solve this problem [3], [16–19]. The models given in [16], [19] have boundary lock issues and the polarity-dependent window functions given in [17], [19] are

DOI: 10.13164/re.2023.0312

developed to overcome the problem. Chua has diagnosed resistive memories as memristive systems [7]. Even if a memristor's power is cut off, the memristor remembers its last resistance value and starts from the resistance value when it is repowered [1], [3]. A memristor does not dissipate power if its current is zero. That's why one of the most important memristive system applications is Non-Volatile Random Access Memory (NVRAM) applications [5–10]. ReRAM application of the TiO_2-based memristors is reviewed in [20]. It is possible to make low-power dissipating high-density memristor-based SRAMs [21]. The ReRAM structure has been first discovered with nickel oxide (NiO) in 1964 [22]. There are various materials suitable to make resistive memories [23–29]. The following examples are just some of them. Silicon oxide has been used to make resistive memories [23]. The conducting nanofilaments within a Pt/TiO_2/Pt system during resistive switching have been probed in [24]. Memristive switching mechanism for metal/oxide/metal nanodevices has been examined in [25]. Both bipolar and unipolar ReRAM operations have been reviewed in [26]. A coarse-grained classification into primarily thermal, electrical, or ion-migration-induced switching mechanisms has been proposed in [27]. Atomic force microscopy studies done in [28] under different vacuum conditions demonstrated that resistance switching is closely related to the formation and removal of conducting spots. Testing results given in [29] show that Si or Al implantation into HfO_2 films results in reduced electroforming voltages and improves the reproducibility of resistive switching. The effects of the thickness dependence and electrode size on the resistive switching characteristics of the ZrO_2 have been examined in [30]. Resistive switching of NiO films has been examined in [22]. Resistive switching of the Complementary Resistive Switches and their application to passive nano crossbar memories for power consumption reduction have been examined in [31]. The vertical integration of Complementary Resistive Switch cells based on Cu/SiO_2/Pt bipolar resistive switches has been demonstrated in [32]. Using CRS-based memristors lets 3D stacking crossbar memories have less leakage current [33]. Such CRS-based memories may need reconstructive circuits [34]. Memristive materials can also be used in digital circuit applications. Memristor-based digital circuits such as reconfigurable logic circuits, flip-flops, latches, etc. are also examined in the literature [35–41]. It is possible to make memristor-based programmable logic circuits [34]. Memristor-based flip-flop circuits are nonvolatile and dissipate low power [36], [37]. They allow the making of reconfigurable logic gates and devices [38], [39]. Such memristor-based logic and memory circuits may require adaptive writing circuits [40]. A review of the memristor-based logic circuit design can be found in [41]. The change of the resistance of a memristor from R_{on} to R_{off} or from R_{off} to R_{on} under the applied voltage or with current flowing through it is called "memristive switching" or "resistive switching" [42]. The time required for this is called the "memristive or the resistive switching time". Writing or deleting memristor-based memories or memristor-based digital applications aforementioned require memristive switching to occur. That's why the memristive or resistive switching time is an important parameter to evaluate the performance of the memristor-based computer memories and digital circuits [8, 11, 31, 34, 38, 39, 42, 43]. Memristive switching time has been studied conceptually and experimentally using a piecewise linear charge-flux characteristic in [42]. This time value may differ concerning the direction of current or voltage [17], [19]. In [44], the effect of delayed memristive switching to memristor-based artificial neural networks has been investigated analytically and experimentally. In the studies given in [45], [46], the memristive switching time is calculated using the HP memristor model. In [47], it is claimed that memristive switching could be used to calculate the memristance function. The memristive switching time is an important parameter due to the aforementioned applications. It should be calculatable using the memristor device parameters and the memristor model used. In this study, first, the memristive switching time formula for nonlinear drift speed memristor models is derived and, then, the memristive switching times of the models given in [3], [16–19] are tried to be calculated using their window functions for both polarities. The WolframAlpha program is used for the complex integrals used to calculate the switching times. The integrals are found to diverge. The results of integrals are interpreted. A new memristor model with a finite switching time is proposed.

This study is organized as follows. In Sec. 2, a brief introduction to the nonlinear dopant drift memristor models is given, and the window functions of these memristor models are briefly explained. In Sec. 3, the formula to calculate the memristive switching time for both of the current polarities is derived Analytical solutions of the switching times of the nonlinear dopant drift memristor models are sought in Sec. 4. A new memristor window function is proposed, its switching time for both polarities are calculated, and the new model is compared with the other memristor models used in this study in Sec. 5. Two examples of the model usage are given in Sec. 6. The paper is concluded with the conclusion section.

2. Memristor Models and Their Window Functions

In this section, the memristor models used in this study are briefly explained. An (ideal) memristor is a special case of the memristive systems [2], in which the state variable of the memristive system is the memristor charge. However, the thin-film systems, which are actually memristive systems, are also called memristors nowadays [48]. Such a memristor model with nonlinear dopant drift is given as

$$v(t) = R(x) \cdot i(t), \tag{1}$$

$$\frac{\mathrm{d}x}{\mathrm{d}t} = \mu_v \frac{R_{on}}{D^2} \cdot i(t) f(x,i) \tag{2}$$

where $R(x)$ is the memristor resistance, $i(t)$ is its current, $v(t)$ is its voltage, D is the total length of TiO_2 region, x is the memristor state variable, μ_v is its dopant mobility, R_{on} is its

minimum resistance, $f(x,i)$ is its polarity-dependent window function, often written as $f(x)$ in the literature.

The memristor state variable, which is its normalized oxidized length, can be expressed as

$$x = w/D \tag{3}$$

where w is its instant oxidized length.

A window function is added to such a memristor model to determine the drift speed rate by multiplying the memristor current as shown in (2) [3], [16–19]. The memristor resistance is given as

$$R(x) = R_{on}x + R_{off}(1-x) = R_{off} - (R_{off} - R_{on}) \cdot x. \tag{4}$$

According to the model in [3], its resistance ranges from its minimum value R_{on} to its maximum value R_{off}. Therefore, for the resistance of a memristor, this is always true:

$$R_{off} \geq R(x) \geq R_{on}. \tag{5}$$

In this study, Strukov [3], Joglekar [16], Biolek [17], Prodromakis [18], and Zha memristor [19] models are used. A review of the memristor models used in this study can be found in [49]. These models have window functions and a window function is a measure of how much a memristor approaches being an ideal memristor [17]. These window functions are given in Tab. 1. Polarity-dependent window functions are written as $f(x)$ in the literature but the polarity-dependent window functions are written as $f(x,i)$ in this study. Their resistance value or memristive state variable starts changing only when both their window function and current are different from zero. The window functions in [16], [18], that have zero dopant speeds at the memristive layer boundaries, possess a problem called the boundary lock issue: at $x = 0$ and $x = 1$, their resistance value or memristive state-variable or window function $f(x)$ does not change whatever the current is. The models in [17] and [19] do not suffer from the issues. These window functions given in Tab. 1 are all phenomenal functions. The experimental data may pave the way to more realistic window functions with better accuracy in the future. HP model's window function can be taken as equal to 1 [3]. stp() in Tab. 1 is the unit step function and is given as

$$\text{stp}(i) = \begin{cases} 1, & i \geq 0, \\ 0, & i < 0. \end{cases} \tag{6}$$

Comparisons of the mentioned window functions, whose resistive switching time is examined in this study, is given in Tab. 2. Strukov model has a quadratic window function, which is not scalable and it has a boundary lock problem, i.e., once the boundary is reached, the regions get locked to the boundaries, and the model starts behaving as a resistor and even changing the polarity cannot solve the problem since $f(1) = f(0) = 0$. The window function of Joglekar model has a shaping parameter (p) and that's why its shape can be modified with it but it also has a boundary lock issue. Biolek model has a current polarity-dependent window function. For $i > 0$, $f(1) = 0$, the memristor behaves as an LTI resistor. However, for $i < 0$, $f(1) = 1$, i.e., the resistance of the memristor starts varying. For $i < 0$, $f(0) = 0$, the memristor behaves as a resistor. However, for $i \geq 0$, $f(0) = 1$, i.e., the resistance of the memristor starts varying. Changing the current polarity of the model results in changing the resistance of the model and that's why the model does not have any boundary lock problems. However, the model is not scalable. Prodromakis model has a boundary lock problem but its window function is scalable with the parameter j. Zha model combines the polarity dependency of Biolek's window function and the scalability of Prodromakis' window function.

The model	Its window function $f(x)$ or $f(x,i)$
HP	$f(x) = 1$
Strukov	$f(x) = x - x^2$
Joglekar	$f(x) = 1 - (2x - 1)^{2p}$
Biolek	$f(x,i) = 1 - (x - \text{stp}(-i(t)))^{2p}$
Prodromakis	$f(x) = j(1 - ((x - 0.5)^2 + 0.75)^p)$
Zha	$f(x,i) = j(1 - (0.25\,(x - \text{stp}(-i))^2 + 0.75)^p)$

Tab. 1. The memristor window functions used in this study.

Window functions	Strukov	Joglekar	Biolek	Prodromakis	Zha
Variables	x	x	x,i	x	x,i
Formability	No	Yes	Yes	Yes	Yes
Formability parameter	-	p	p	p	p
Scalability	No	No	No	Yes	Yes
Scalability parameter	-	-	-	j	j
Boundary lock problem	Yes	Yes	No	Yes	No

Tab. 2. Comparison of the properties of the window functions, whose resistive switching times are examined in this study.

3. Derivation of Resistive Switching Time Formula of Nonlinear Dopant Drift Memristive Models

The circuits, which are used to examine memristive switching, are shown in Fig. 1. The circuit in Fig. 1(a) has a positive DC voltage source and the switch is turned on at a time equal to zero. Assuming the memristor resistance is equal to R_{off} at $t = 0$, the memristor resistance falls down from R_{off} to R_{on}. In Fig. 1(b), a negative DC voltage is applied to the memristor at $t = 0$, assuming that the memristor resistance is equal to R_{on}, the memristor resistance rises from R_{on} to R_{off}. For memristor models depending on the direction of the current, the memristive switching time should be calculated for both polarities.

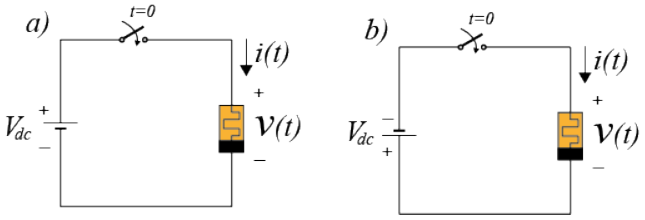

Fig. 1. (a) Memristor fed by a positive DC voltage source (forward-biased memristor) for resistive switching from R_{off} to R_{on}. (b) Memristor fed by a negative DC voltage source (reverse-biased memristor) for resistive switching from R_{on} to R_{off}.

For the memristor models given in the last section, the memristive switching time can be calculated as follows. For a forward-biased memristor, the memristor current for a constant voltage V_{dc} is

$$i(t)=\frac{v(t)}{R(x)}=\frac{V_{dc}}{R(x)}. \tag{7}$$

Then, the derivative of the state variable of the memristive models can be written as

$$\frac{dx}{dt}=\frac{\mu_V R_{on}}{D^2}i(t)f(x)=\frac{\mu_V R_{on}V_{dc}f(x)}{D^2R(x)}. \tag{8}$$

By rearranging (8),

$$dt=\frac{D^2R(x)dx}{\mu_V R_{on}V_{dc}f(x)}. \tag{9}$$

For a forward-biased memristor, the complete resistive switching time, in which x goes up from 0 to 1, is found as

$$\begin{aligned}\tau_{SW}&=\int_0^{\tau_{SW}}dt=\frac{D^2}{\mu_V R_{on}V_{dc}}\int_0^1\frac{R(x)dx}{f(x)}\\&=\frac{D^2}{\mu_V R_{on}V_{dc}}\int_0^1\frac{\left(R_{off}x+R_{on}(1-x)\right)dx}{f(x)}.\end{aligned} \tag{10}$$

For a reverse-biased memristor, the switching voltage is negative and equal to $-V_{dc}$, the complete resistive switching time, in which x goes down from 1 to 0, is found as

$$\begin{aligned}\tau_{SW}&=\int_0^{\tau_{SW}}dt=\frac{D^2}{\mu_V R_{on}(-V_{dc})}\int_1^0\frac{R(x)dx}{f(x)}\\&=\frac{D^2}{\mu_V R_{on}V_{dc}}\int_0^1\frac{R(x)dx}{f(x)}.\end{aligned} \tag{11}$$

Equation (11) is the same as (10). However, the window function must be used correctly with the proper polarity in these equations.

4. Examination of Memristive Switching Time of Nonlinear Dopant Drift Memristive Models

Now, the switching time of the models summarized in the last section can be calculated using the equation given in the last section.

4.1 Resistive Switching Time of HP Memristor Model

HP memristor model is the first and the simplest memristor model and it is made under the assumption that linear dopant drift exists in the memristive element [3]. The window function of an HP memristor can be taken as equal to 1, i.e., $f(x) = 1$. The memristive switching of an HP memristor can be found as

$$\tau_{SW}=\frac{D^2}{\mu_V R_{on}V_{dc}}\left[R_{off}x+\frac{(R_{on}-R_{off})x^2}{2}\right]_0^1=\frac{D^2(R_{on}+R_{off})}{2\mu_V R_{on}V_{dc}}. \tag{12}$$

The memristive switching time of an HP memristor for positive and negative polarities is the same and is given by (12). For an HP memristor, the memristive switching time is inversely proportional to the DC voltage applied. The memristor parameters, D, μ_V, R_{on}, and R_{off}, and the switching voltage V_{dc} define the memristive switching time under DC excitation for a complete resistive switching. The higher the ratio of the maximum resistance to the minimum resistance, the higher the memristive switching time.

4.2 Resistive Switching Time of the Memristor Model with Strukov Window Function

Strukov window function is not dependent on current polarity and is given as

$$f(x)=x-x^2. \tag{13}$$

That's why its memristive switching time are the same in the reverse-biased and forward-biased memristor. Its memristive switching time can be calculated as

$$\tau_{SW}=\frac{1}{V_{dc}K}\left(R_{on}\cdot\int_0^1\frac{x}{x(1-x)}dx+R_{off}\cdot\int_0^1\frac{(1-x)}{x(1-x)}dx\right), \tag{14}$$

$$\tau_{SW}=\frac{1}{V_{dc}K}\left(R_{on}\ln|1-x|\Big|_0^1+R_{off}\ln|x|\Big|_0^1\right)=\infty. \tag{15}$$

The memristive switching time of the model is infinite or the integral does not converge. This is expected since the model has a boundary lock problem. At the boundaries, at $x = 0$ and $x = 1$, the rate of the change of the state variable $x(t)$ is zero since the window function is also zero at the boundaries, i.e., $f(0) = f(1) = 0$. That's why the model cannot do switching.

4.3 Resistive Switching Time of the Memristor Model with Joglekar Window Function

Joglekar window function is also not dependent on current polarity and is given as

$$f(x)=1-(2x-1)^{2p}. \tag{16}$$

That's why its memristive switching time are the same in the reverse- and forward-biased memristor. Using Wolfram-Alpha for the integration, its memristive switching time can be calculated as

$$\begin{aligned}\tau_{\mathrm{SW}} &= \frac{1}{V_{\mathrm{dc}}K}\int_0^1 \frac{R(x)}{1-(2x-1)^{2p}}\,\mathrm{d}x \\ &= \frac{1}{V_{\mathrm{dc}}K}\int_0^1 \frac{R_{\mathrm{on}}\cdot x+R_{\mathrm{off}}\cdot(1-x)}{1-(2x-1)^{2p}}\,\mathrm{d}x=\infty.\end{aligned} \tag{17}$$

The memristive switching time of the model is also infinite or the integral does not converge. This is expected since the model has also a boundary lock problem.

4.4 Resistive Switching Time of the Memristor Model with Biolek Window Function

Biolek function is dependent on current polarity and is given as

$$f(x)=1-\left(x-\mathrm{stp}\left(-i(t)\right)\right)^{2p}. \tag{18}$$

That's why its memristive switching time are not the same in the reverse- and forward-biased memristor. Its memristive switching time can be calculated as

$$\tau_{\mathrm{SW}}=\frac{1}{V_{\mathrm{dc}}K}\int_0^1 \frac{R(x)}{1-\left(x-\mathrm{stp}\left(-i(t)\right)\right)^{2p}}\,\mathrm{d}x. \tag{19}$$

Using Wolfram-Alpha integral calculator, for the forward-biased polarity, $i(t) \geq 0$, the forward-biased switching time

$$\tau_{\mathrm{SW}}=\frac{1}{V_{\mathrm{dc}}K}\int_0^1 \frac{R_{\mathrm{on}}\cdot x+R_{\mathrm{off}}\cdot(1-x)}{1-(x)^{2p}}\,\mathrm{d}x=\infty. \tag{20}$$

For the forward-biased polarity, the memristive switching time of the model is found also infinite or the integral does not converge. This is not expected since the model does not have any boundary lock problems.

Using Wolfram-Alpha integral calculator, for the reverse-biased polarity, $i(t) < 0$, the reverse-biased switching time

$$\tau_{\mathrm{SW}}=\frac{1}{V_{\mathrm{dc}}K}\int_0^1 \frac{R_{\mathrm{on}}\cdot x+R_{\mathrm{off}}\cdot(1-x)}{1-(x-1)^{2p}}\,\mathrm{d}x=\infty. \tag{21}$$

For the reverse-biased polarity, the memristive switching time of the model is also infinite or the integral does not converge. This is not expected since the model does not have any boundary lock problems. The doped region within the memristor is unable to reach the boundary. This new problem is called "the boundary unreachability problem" in this study.

4.5 Resistive Switching Time of the Memristor Model with Prodromakis Window Function

Prodromakis window function is also not dependent on current polarity and is given as

$$f(x)=j\left(1-\left((x-0.5)^2+0.75\right)^p\right). \tag{22}$$

That's why its memristive switching time are the same in the reverse-biased and forward-biased memristor. Using Wolfram-Alpha integral calculator, its memristive switching time can be calculated as

$$\tau_{\mathrm{SW}}=\frac{1}{V_{\mathrm{dc}}Kj}\int_0^1 \frac{R(x)}{\left(1-\left((x-0.5)^2+0.75\right)^p\right)}\,\mathrm{d}x=\infty. \tag{23}$$

The integral does not converge. Therefore, the switching time of the memristor model is infinite since it is also expected due to the model's boundary lock problem.

4.6 Resistive Switching Time of the Memristor Model with Zha Window Function

Zha window function is dependent on current polarity and is given as

$$f(x)=j\left(1-\left(0.25\left(x-\mathrm{stp}\left(-i\right)\right)^2+0.75\right)^p\right). \tag{24}$$

That's why its memristive switching time are not the same in the reverse-biased and forward-biased memristor. Its memristive switching time can be calculated as

$$\tau_{\mathrm{SW}}=\frac{1}{V_{\mathrm{dc}}Kj}\int_0^1 \frac{R(x)}{1-\left(0.25\left(x-\mathrm{stp}\left(-i\right)\right)^2+0.75\right)^p}\,\mathrm{d}x. \tag{25}$$

Using Wolfram-Alpha integral calculator, for the forward-biased polarity, $i(t) \geq 0$, the forward-biased switching time

$$\tau_{\mathrm{SW}}=\frac{1}{V_{\mathrm{dc}}Kj}\int_0^1 \frac{R_{\mathrm{on}}\cdot x+R_{\mathrm{off}}\cdot(1-x)}{1-\left(0.25x^2+0.75\right)^p}\,\mathrm{d}x=\infty\cdot \tag{26}$$

The integral does not converge. Using Wolfram-Alpha integral calculator, for the reverse-biased polarity, $i(t) < 0$, the reverse-biased switching time

$$\tau_{\mathrm{SW}}=\frac{1}{V_{\mathrm{dc}}Kj}\int_0^1 \frac{R_{\mathrm{on}}\cdot x+R_{\mathrm{off}}\cdot(1-x)}{1-\left(0.25\left(x-1\right)^2+0.75\right)^p}\,\mathrm{d}x=\infty. \tag{27}$$

For both polarities, the integrals do not converge and, therefore, the memristive switching time of the model is infinite. This is not expected since the model does not have any boundary lock problems. Zha model also has "the boundary unreachability problem".

5. A New Window Function Suggestion and its Switching Time Calculation

In the previous section, a new shortcoming of these phenomenological memristor models has been shown that their switching times go to infinity, i.e., they cannot do memristive switching. Biolek and Zha model has the problem of the doped region within the memristive element not reaching the boundaries for both polarities of the current. As the doped region approaches any of the boundaries ($x = 0$ or $x = 1$) under constant voltage, the doped region slows down so much that the switching time becomes infinite, that is, it cannot reach the limit in a finite time. This is a modern Zeno paradox [50]. In other words, these and perhaps some other memristor models in the literature are not physical. Therefore, new memristor models with convergent switching times are needed for a more accurate physical modeling. Such models may help to better understand the charge mobility within a memristor and the physical mechanism of the respective memristor system. In this section, a new window function to overcome the boundary lock and boundary unreachability issues is proposed and its switching time is calculated and shown to be finite. The following new window function, which is also polarity dependent, is proposed:

$$f(x,i) = m_1 \sqrt[n]{1-x} \cdot \mathrm{stp}(i) + m_2 \sqrt[n]{x} \cdot \mathrm{stp}(-i) \tag{28}$$

where n is a positive number, which does not have to be an integer, m_1 is the scaling coefficient in the forward direction, m_2 is the scaling coefficient in the reverse direction, i is the memristor current, and stp() is the unit step function.

The function $f(x,i)$ considering current polarity can be written as the following piece-wise function:

$$f(x,i) = \begin{cases} m_1 \sqrt[n]{1-x}, & i \geq 0, \\ m_2 \sqrt[n]{x}, & i < 0. \end{cases} \tag{29}$$

The memristor model with the new window function can be expressed as

$$v(t) = R(x) \cdot i(t), \tag{30}$$

$$\frac{\mathrm{d}x}{\mathrm{d}t} = \mu_v \frac{R_{on}}{D^2} \cdot i(t) f(x,i) = K \cdot i(t) f(x,i), \tag{31}$$

$$f(x,i) = \begin{cases} m_1 \sqrt[n]{1-x}, & i \geq 0, \\ m_2 \sqrt[n]{x}, & i < 0, \end{cases} \tag{32}$$

$$R(x) = R_{on} x + R_{off}(1-x). \tag{33}$$

The parameters of the model can be found using curve-fitting to the experimental data. The minimum and maximum value of the memristor resistance can be found easily applying a square-wave to the memristor as done in [47]. Using the negative and positive half period sections of the memristor voltage and current waveforms and the resistive switching formulas derived here, K, m_1, and m_2 can be found. Implementing the model in programs such as Matlab/Simulink or LTspice is pretty easy.

For the reverse polarity, i.e., $i(t) < 0$, the memristive switching time:

$$\begin{aligned} \tau_{SW} &= \int_0^1 \frac{R(x)\,\mathrm{d}x}{V_{dc} K m_2 \sqrt[n]{x}} \\ &= \frac{1}{V_{dc} K} \left(\frac{R_{on} - R_{off}}{m_2} \int_0^1 \frac{x}{\sqrt[n]{x}} \mathrm{d}x + \frac{R_{off}}{m_2} \int_0^1 \frac{1}{\sqrt[n]{x}} \mathrm{d}x \right). \end{aligned} \tag{34}$$

Submitting $\frac{x}{\sqrt[n]{x}} = x^{n-1/n}$ to (30) and remembering $\int x^a \mathrm{d}x = \frac{x^{a+1}}{a+1}, a \neq 1$:

$$\tau_{SW} = \frac{1}{V_{dc} K} \left(\frac{R_{on} - R_{off}}{m_2} \left(\frac{n}{2n-1} \right) + \frac{R_{off}}{m_2} \left(\frac{n}{n-1} \right) \right). \tag{35}$$

From (35), it can be seen that the switching time converges except for $n = ½$ and $n = 1$. This shows that this memristor model switches in a finite time or is able to do memristive switching under negative DC voltage. Therefore, the model is physically more accurate. However, the model has also its limits: the switching time cannot be negative. For $n < 1$, if $(R_{on} - R_{off})n / (2n - 1) > R_{off} n / (n - 1)$, the switching time becomes negative since $(R_{on} - R_{off})$ is negative. For $n > 1$, the switching time is always positive that is more desirable.

The graph of the new window function for the reverse polarity and $m_2 = 1$ is given in Fig. 2. The parameter n allows the window function to be shaped. The function increases rapidly starting from zero at $x = 0$ for $n > 1$ values. For $n = 20$, it starts to resemble almost a line after a rapid rise. It can be said that as the value of n increases further, it will take an almost constant value after a rapid rise. For $n < 1$, as the value of n decreases, the shape of the curve resembles a parabola first, it deviates from being a parabola as it approaches the $x = 1$ boundary, and it rises rapidly resembling the characteristic of a diode operating in the conduction region. As it can be seen from the rightmost curve for $n = 1/50$ or for very small values of n, the window function first increases very slowly and, then, increases rapidly as it approaches the $x = 1$ boundary. It should be remembered that the curves with $n > 1$ is more desirable.

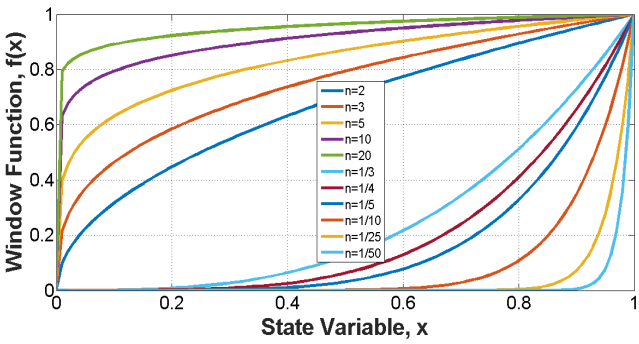

Fig. 2. The newly proposed window function for the reverse biased memristor ($i(t) < 0$), various n values, and $m_2 = 1$.

For the forward biased memristor or the forward polarity, i.e., $i(t) \geq 0$, the memristive switching time can be calculated as

$$\tau_{SW} = \int_0^1 \frac{R(x)\,dx}{V_{dc} K m_1 \sqrt[n]{1-x}} = \left(\frac{R_{on} - R_{off}}{V_{dc} K m_1}\right)\left(\frac{n}{2n-1}\right) + \frac{R_{off}}{V_{dc} K m_1}\left(\frac{n}{n-1}\right). \quad (36)$$

From (36), it can be seen that the switching time converges except for $n = ½$ and $n = 1$. This shows that this memristor model switches in a finite time or able to do memristive switching under positive DC voltage. Therefore, the model is physically more accurate. However, the model has also its limits: the switching time cannot be negative. For $n < ½$, the switching time is not always positive for all possible R_{on} and R_{off} values. For $n > 1$values, the switching time of the forward-biased memristor is always positive as it is the case for the reverse-biased memristor. Therefore, it is best to use this window function to model a physical memristor system for $n > 1$. The graph of the new window function for the reverse polarity and $m_1 = 1$ is given in Fig. 3. As the function approaches the limit of $x = 1$ for $n > 1$ and high n values, it decreases monotonously and becomes zero. For $n = 20$, it resembles an almost linear curve, and, when it approaches the limit of $x = 1$, it becomes zero following a rapid decline. For $n < 1$ values, the shape of the window function resembles a capacitor discharge curve. As the value of n decreases, the rate of decline of the curve around $x = 0$ gradually increases. As can be seen from the leftmost curve for $n = 1/50$ or for very low n values, it first decreases very rapidly, starting from the value 1, and then slowly decreases until it reaches $x = 1$, and it becomes zero at $x = 1$. It should be remembered that the curves with $n > 1$ are more desirable. The comparison of other memristor window functions used in this study with the newly proposed window function is given in Tab. 3.

In the new model, the current variable i is used together with the state variable x as in the Biolek and Zha models. Thus, the problem of boundary lock seen in the Strukov, Joglekar and Prodromakis models has been avoided. The boundary unreachability problem, which exists in Biolek and Zha models, has also been resolved in this new model since it has a finite switching time in both polarities, which is the best advantage of the proposed memristor model. The

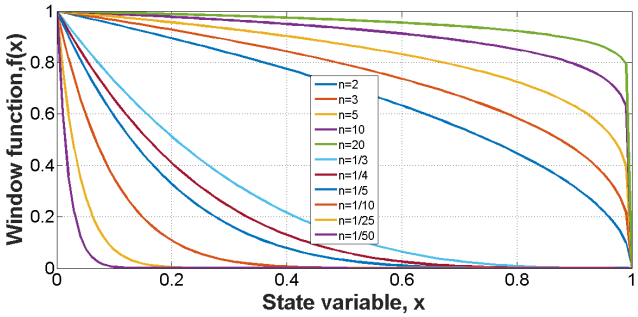

Fig. 3. The newly proposed window function for the forward biased memristor ($i(t) > 0$), various n values, and $m_1 = 1$.

Window functions	Strukov	Joglekar	Biolek	Prodromakis	Zha	The new model
Variables of the window function	x	x	x, i	x	x, i	x, i
Formability	No	Yes	Yes	Yes	Yes	Yes
Formability parameter	-	p	p	p	p	n
Scalability	No	No	No	Yes	Yes	Yes
Scalability parameter	-	-	-	j	j	m_1, m_2
Problem of boundary lock	Yes	Yes	No	Yes	No	No
Boundary unreachability	No	No	Yes	No	Yes	No

Tab. 3. Comparison of the memristor window functions used in this study and the newly proposed window function.

window function of the memristor model can also be shaped with the parameter n and be scaled with the parameters m_1 and m_2. Only two of the examined models have a scaling parameter j and the rest of the models lack one as seen in Tab. 3. The proposed window function having two scaling parameters can be scaled separately for each polarity, which can allow a better fitting to experimental data, and the other models do not possess the double scalability property, either. For some $n < 1$ values, this new model gives a negative switching time in the forward direction. Therefore, this window function cannot be used to model memristor for every n value.

6. Analytical and Simulation Examples for the Proposed Model

Comprehension of how to use the proposed memristor model is of importance. That's why, in this section, analytical and simulation examples of its usage are given.

As a first example, the time domain response of the new memristor model for a DC voltage is also examined for the reverse polarity, i.e., $v(t) = -V_{dc}$ and $i(t) < 0$. By taking the integration of both sides of (9), its solution can be found as:

$$t = \frac{1}{V_{dc} K}\left(\frac{R_{on} - R_{off}}{m_2}\int_{x(0)}^{x(t)} x^{1-1/n}\,dx + \frac{R_{off}}{m_2}\int_{x(0)}^{x(t)} x^{-1/n}\,dx\right), \quad (37)$$

$$t = \frac{R_{on} - R_{off}}{V_{dc} K m_2\left(2 - \frac{1}{n}\right)}\left(x(t)^{2-\frac{1}{n}} - x(0)^{2-\frac{1}{n}}\right) + \frac{R_{off}}{V_{dc} K m_2\left(1 - \frac{1}{n}\right)}\left(x(t)^{1-\frac{1}{n}} - x(0)^{1-\frac{1}{n}}\right). \quad (38)$$

The solution is in implicit form, i.e., it cannot be expressed as a direct function of t. Equation (38) is still much simpler than the solutions of (9), which can be obtained

using other window functions. Equation (38) does not have an analytical solution. For the high values of n, $1 >> 1/n$, Equation (38) can be approximated as:

$$t \cong \frac{R_{on}-R_{off}}{V_{dc}Km_2\left(2-\frac{1}{n}\right)}\left(x(t)^2-x(0)^2\right) + \frac{R_{off}}{V_{dc}Km_2\left(1-\frac{1}{n}\right)}\left(x(t)-x(0)\right), \tag{39}$$

$$t = A\left(x(t)^2-x(0)^2\right)+B\left(x(t)-x(0)\right) \tag{40}$$

where $A=\frac{R_{on}-R_{off}}{V_{dc}Km_2\left(2-\frac{1}{n}\right)}$ and $B=\frac{R_{off}}{V_{dc}Km_2\left(1-\frac{1}{n}\right)}$.

Equation (40) can be solved since it is a quadratic equation. Rearranging (40),

$$Ax(t)^2+Bx(t)-Ax(0)^2-Bx(0)-t=0. \tag{41}$$

Equation (40) has two roots but the negative solution is disregarded since only $x(t) \geq 0$ is physical. Therefore, its solution is given as

$$x(t)=\frac{-B+\sqrt{B^2+4A\left(Ax(0)^2+Bx(0)+t\right)}}{2A}. \tag{42}$$

Equation (42) is valid for $t \leq \tau_{SW}$. Substituting (42) into (4) and (7), the memristance and current of the memristor can be found as:

$$R(x) \cong R_{off}-\left(R_{off}-R_{on}\right)\frac{-B+\sqrt{C+4At}}{2A}, \tag{43}$$

$$i(t) \cong -\frac{V_{dc}}{R(x)}=-\frac{V_{dc}}{R_{off}-\left(R_{off}-R_{on}\right)\frac{-B+\sqrt{C+4At}}{2A}} \tag{44}$$

where $C=\sqrt{B^2+4A^2x(0)^2+4ABx(0)}$.

After the switching occurs in the reverse direction, i.e. for $t \geq \tau_{SW}$,

$$x(t)=0, \tag{45}$$

$$R(x)=R_{off}, \tag{46}$$

$$i(t)=-\frac{V_{dc}}{R(x)}=-\frac{V_{dc}}{R_{off}}. \tag{47}$$

The perturbation theory can also be used to solve (38) more accurately assuming $(1/n)$ is a small parameter but the solution is not sought further. $x(t)$ can also be solved numerically if desired. The time domain response of the new memristor model for a DC voltage can also be examined similarly for the forward polarity, due to space considerations, it is not examined in this paper.

The frequency domain response of the new memristor model for a DC voltage is also examined for the reverse polarity. By taking the Fourier transformation of (42), the state variable of the memristor in frequency domain can be found as:

$$x(\omega)=\int_0^{\infty}x(t)\,e^{-i\omega t}\,dt. \tag{48}$$

Using the approximate solution, (43), for a pulse width of T_P shorter than or equal to the reverse switching time τ_{SW}, i.e., $0 \leq t \leq T_P \leq \tau_{SW}$, Equation (49) turns into:

$$x(\omega) \cong \int_0^{T_P}\frac{-B+\sqrt{C+4At}}{2A}e^{-i\omega t}dt. \tag{49}$$

Using the approximate solution, (43), for $t \leq \tau_{SW}$, Equation (48) turns into:

$$x(\omega) \cong \frac{i\,e^{-i\omega T_P}}{4A\omega^{\frac{3}{2}}}\left(\begin{array}{l}2\sqrt{\omega}\left(-B+\sqrt{C+4AT_P}\right)+\\(-1)^{\frac{3}{4}}\sqrt{4\pi A}\,e^{-\frac{i\omega(C+4AT_P)}{4A}}+\\\operatorname{erf}\left(\frac{(-1)^{\frac{1}{4}}\sqrt{\omega}\sqrt{C+4AT_P}}{\sqrt{4A}}\right)\end{array}\right) - \frac{i\left(-B+\sqrt{C}\right)}{2A\omega}-\frac{i\sqrt{\frac{\pi}{4A}}(-1)^{\frac{3}{4}}}{\omega^{\frac{3}{2}}}e^{-\frac{i\omega C}{4A}} - \frac{i\cdot\operatorname{erf}\left((-1)^{\frac{1}{4}}\sqrt{\frac{\omega C}{4A}}\right)}{4A\omega^{\frac{3}{2}}} \tag{50}$$

where erf(y) is the error function and it is given as:

$$\operatorname{erf}(y)=\frac{2}{\sqrt{\pi}}\int_0^{y}e^{-u^2}\,du. \tag{51}$$

Using the approximate solution, (42), for a pulse width of T_P higher than or equal to the reverse switching time τ_{SW}, i.e., $T_P > \tau_{SW} \geq t \geq 0$, Equation (48) turns into:

$$x(\omega) \cong \int_0^{\tau_{SW}}\frac{-B+\sqrt{B^2+4A\left(Ax(0)^2+Bx(0)+t\right)}}{2A}e^{-i\omega t}\,dt + \int_{\tau_{SW}}^{T_P}0\cdot e^{-i\omega t}\,dt, \tag{52}$$

$$x(\omega)\cong\frac{\mathrm{i}\,\mathrm{e}^{-\mathrm{i}\omega\tau_{\mathrm{SW}}}}{4A\omega^{\frac{3}{2}}}\left(\begin{array}{l}2\sqrt{\omega}\left(-B+\sqrt{C+4A\tau_{\mathrm{SW}}}\right)\\+(-1)^{\frac{3}{4}}\sqrt{4\pi A}\,\mathrm{e}^{\frac{\mathrm{i}\omega(C+4A\tau_{\mathrm{SW}})}{4A}}\\+\mathrm{erf}\left(\dfrac{(-1)^{\frac{1}{4}}\sqrt{\omega}\sqrt{C+4A\tau_{\mathrm{SW}}}}{\sqrt{4A}}\right)\end{array}\right)\qquad(53)$$

$$-\frac{i\left(-B+\sqrt{C}\right)}{2A\omega}-\frac{\mathrm{i}\sqrt{\dfrac{\pi}{4A}}(-1)^{\frac{3}{4}}}{\omega^{\frac{3}{2}}}\mathrm{e}^{\frac{\mathrm{i}\omega C}{4A}}-\frac{\mathrm{i}\cdot\mathrm{erf}\left((-1)^{\frac{1}{4}}\sqrt{\dfrac{\omega C}{4A}}\right)}{4A\omega^{\frac{3}{2}}}$$

where $\tau_{\mathrm{SW}}=\dfrac{1}{V_{\mathrm{dc}}K}\left(\dfrac{R_{\mathrm{on}}-R_{\mathrm{off}}}{m_2}\left(\dfrac{n}{2n-1}\right)+\dfrac{R_{\mathrm{off}}}{m_2}\left(\dfrac{n}{n-1}\right)\right)$.

The frequency domain response of the new memristor model for a DC voltage can also be examined similarly for the forward polarity, due to space considerations, it is not examined in this paper.

As a second example of the model's usage, LTspice model of the proposed memristor model is used to show its hysteresis behavior and to examine a memristor-capacitor (M-C) parallel circuit. The memristor model is simulated with a sinusoidal voltage for three different frequencies to obtain its hysteresis curves and to demonstrate that it possesses the three fingerprints of a memristor as seen in Fig. 4. The hysteresis curves of the memristor are not symmetric with respect to the origin due to its polarity dependence and having different scalability factors. Recently, an M-C circuit which is shown in Fig. 5 has been examined in [51]. Such M-C circuits may be used to obtain characteristics of a memristor, to analyze some device configurations with a memristor and a capacitor [51], be of importance to model biological systems, and can be used as a memristor test similar to the one given in [52]. In such a circuit, a complete resistive switching cannot occur in a memristor modeled with a boundary unreachability problem for any initial charge of the capacitor. However, a complete resistive switching can occur in a memristor without a boundary unreachability problem for the same initial conditions. If the experimental results show that such a system has a finite resistive switching time, such a system should be modeled with a memristor model without a boundary unreachability problem, perhaps with the one given here or a similar one. Otherwise, if the state variable behaves asymptotically not reaching its upper or lower limits, the models such as the ones given [17], [19] can be used for this purpose. Such an M-C circuit similar to the one given in [51] is simulated using the proposed model given in the last section. The simulation results obtained in LTspice are shown in Fig. 6. The circuit behaves as an M-C circuit at the beginning of the simulation, the memristance starts falling down while the state variable starts going up from $x(0)$ to 1, then, it becomes equal to the minimum memristance value R_{on} at around 0.08 seconds when x becomes equal to 1, it stays constant, and the circuit starts behaving as if an LTI resistor-capacitor circuit

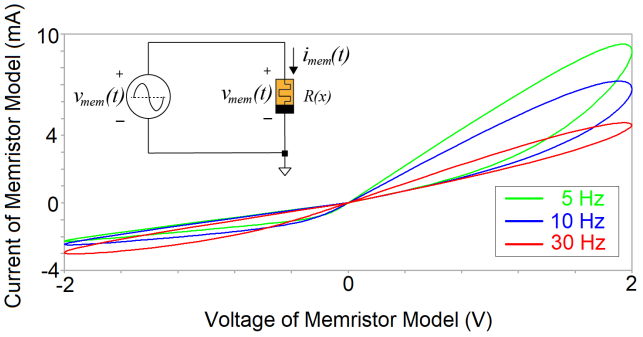

Fig. 4. Hysteresis curves of the simulated memristor fed by a sinusoidal voltage of $v_s(t) = 2{\cdot}\sin(2\pi ft)$ V for the frequencies of 5, 10, and 20 Hz.

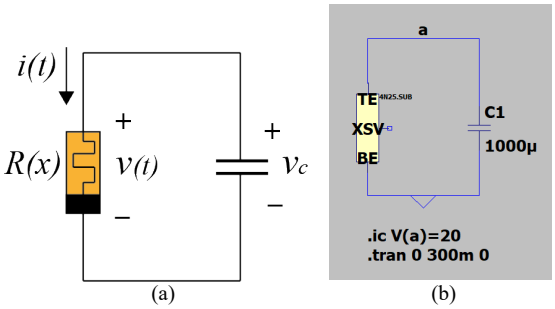

Fig. 5. (a) The M-C circuit examined; (b) Its LTspice schematic.

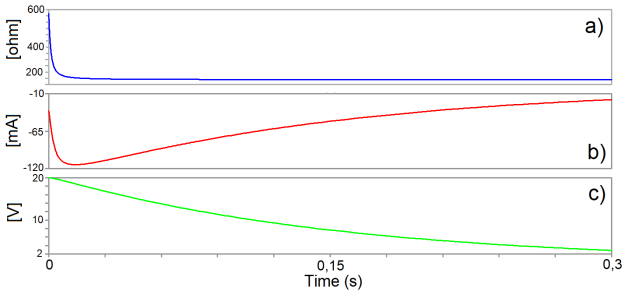

Fig. 6. (a) The memristance, (b) the current, and (c) the voltage, of the forward-biased memristor in the M-C parallel circuit for the simulation parameters, $R_{\mathrm{on}} = 150\ \Omega$, $R_{\mathrm{off}} = 1000\ \Omega$, $x(0) = 0.076$, $D = 16$ nm, $\mu_v = 40 \times 10^{-15}\ \mathrm{m^2/(V{\cdot}s)}$, $p = 7$, $n = 2$, $m_1 = 2$, $m_2 = 3$, $C = 1000\ \mu\mathrm{F}$, and $v_C(0) = 20$ V.

after that. The overall behavior of the M-C circuit is different than that of an LTI resistor-capacitor circuit since it possesses two state variables, $v_c(t)$ and $x(t)$. Its current has a shape similar to a critically-damped R-L-C circuit which is not possible to obtain in an R-C circuit. The M-C circuit with a reverse-polarized memristor would behave differently due to the scaling and shape factors of the model considering (29) but due to space issues, the problem is not examined further. Its analytical examination and how it can be used as a memristor test will be the subject of a future work.

7. Conclusion

Although they are still new products commercially, the resistive memories, which are also memristive systems and

also known as resistive RAM, stand out as a popular field of study in the literature [8]. The switching time of them is an important parameter, which should be calculated accurately, for such a memory application. In this study, the switching time calculations have been made for several well-known memristor models with nonlinear drift speed. Some of these models cannot do memristive switching due to the boundary lock problem. Therefore, the switching times of these models could not be calculated, i.e., when the memristive switching time formula is used, the integration value, which gives the switching time, is found to be infinite or diverging as expected. This confirms that the memristor models with the boundary lock problem cannot do resistive switching. The solutions of the indefinite integrals of the switching times of the memristor models without the boundary lock problem are very complex. By using Wolfram-Alpha integral calculator, which is used for symbolic integration, the integrals giving the switching time are evaluated and calculated. The switching times of the memristor models without the boundary lock problem are also evaluated with Wolfram-Alpha program and surprisingly found to be also infinite, i.e., they also diverge, that is, go to infinity. The reason for this situation has been identified as the drift velocity of the doped region inside the memristor decreases to very low values as it approaches the boundaries in these models and that's why the resistive switching or the total drifting time takes infinite time that can be thought as a modern Zeno's paradox [50]. While the high doped region approaches any of the boundaries under constant voltage, the doped region slows down so much that the switching time becomes infinite, that is, it cannot reach the limit in a finite time, as in Zeno's paradox [50]. That's why this problem is called the boundary unreachability problem or Zeno Problem in this study. Even Biolek model, which is well-known and commonly-used in the literature, and, its improved version, Zha model, have the problem and they cannot do the resistive switching for whatever the switching voltage is. Any memristor model with this problem is not physically correct. Because, according to experimental studies, the ionic memristors can switch in both directions under constant voltage and their switching time decreases with increasing voltage. In the literature, when these memristor models whose switching is examined, are used in simulations in programs such as Spice, LTspice, and Simulink [17], [45], it appears that these memristor models can do resistive switching according to the simulation results. This is because of the fact that the numerical methods used to solve the memristor equation give simulation results with an error. When the switching of these memristors is examined by numerical methods, it seems that the doped region within the memristor has been able to reach any of the boundaries since the doped region moves with the average speed calculated in the previous time but this is not possible as demonstrated in this study. Slowing down of the doped region when approaching to any of the memristor boundaries cannot be modeled or calculated in the numerical methods such as Euler or Runge-Kutta methods due to their discrete nature. Also in this study, the effect of memristor polarity on memristive switching was also investigated, and it has been observed that the switching time integral diverges for both polarities in the nonlinear drift speed memristor models studied. Interestingly, HP memristor model, which is the first memristor model given in the literature, which is now considered obsolete, is the only memristor model whose switching time can be calculated among the memristor models examined in this study. The results show that Biolek's and Zha's memristor models are not physical models despite being numerically simulatable and there is a need for better memristor models, whose memristive switching time integral does converge. In this study, after showing the existence of memristor models with the problem of being unable to do memristive switching or having a Zeno paradox, to overcome this problem, a new memristor model is proposed and it is demonstrated that it does memristive switching in a finite time under DC voltage for both of the polarities. The new model is also compared with the other memristor models. Two examples of the use of the proposed model are given in the paper in Sec. 6. A memristor model must have the three fingerprints of a memristor as explained in [53]. Experimental results such as the ones given in [54] show that a memristor must switch in a finite time but the models examined here analytically cannot do resistive switching in a finite time. That's why, in our opinion, if a memristor model is to be proposed in the literature, the switching time of a memristor model must converge or it must have a finite switching time, this means that the convergence of the memristor switching time integral should also be satisfied as a criterion that such a memristor model must have besides having the three fingerprints of the memristor. The memristor model or other memristor models meeting the criterion given here can be applied to design memristor-based digital circuits and memories more accurately in the future.

The findings of the paper can also be important for communication circuit applications. A memristor whose resistance is around its maximum value is used to make an ultrawide bandwidth receiver [55]. The boundary unreachability problem shown here may have implications for its analytical examination of such a device since its performance cannot be predicted accurately by the simulations done with the memristor models with the boundary unreachability problem. A memristor-based random modulator is made in [56] and it can be examined whether the boundary unreachability problem lets the memristor-based compressive sensing system operate well or not. There are memristor-based AM, ASK, FSK, and BPSK modulators examined in the literature [57–59] and, in our opinion, the performance of such circuits must be inspected considering the boundary unreachability problem and using memristor models without it. Also, modeling of the memristor-based circuits such as filters, amplifiers, and oscillators may suffer from the problem as well and their tuning algorithm may have to be modified accordingly [45, 60, 61]. Perhaps, the window function may also inspire modification or new models of other circuit elements with memory such as memcapacitors or meminductors [62].

Acknowledgments

The authors would like to thank the editors and the anonymous reviewers whose insightful comments have helped to improve the quality of this paper considerably.

References

[1] CHUA, L. O. Memristor – the missing circuit element. *IEEE Transactions on Circuit Theory*, 1971, vol. 18, no. 5, p. 507–519. DOI: 10.1109/TCT.1971.1083337

[2] CHUA, L. O., KANG, S. M. Memristive devices and systems. *Proceedings of the IEEE*, 1976, vol. 64, no. 2, p. 209–223. DOI: 10.1109/PROC.1976.10092

[3] STRUKOV, D. B., SNIDER, G. S., STEWART, D. R., et al. The missing memristor found. *Nature*, 2008, vol. 453, p. 80–83. DOI: 10.1038/nature06932

[4] WILLIAMS, R. S. How we found the missing memristor. *IEEE Spectrum*, 2008, vol. 45, no. 12, p. 28–35. DOI: 10.1109/MSPEC.2008.4687366

[5] PRODROMAKIS, T., TOUMAZOU, C. A review on memristive devices and applications. In *17th IEEE International Conference on Electronics, Circuits and Systems*. Athens (Greece), 2010, p. 934–937. DOI: 10.1109/ICECS.2010.5724666

[6] PERSHIN, Y. V., DI VENTRA, M. Memory effects in complex materials and nanoscale systems. *Advances in Physics*, 2011, vol. 60, no. 2, p. 145–227. DOI: 10.1080/00018732.2010.544961

[7] CHUA, L. O. Resistance switching memories are memristors. *Applied Physics A*, 2011, vol. 102, p. 765–783. DOI: 10.1007/s00339-011-6264-9

[8] DOMARADZKI, J., WOJCIESZAK, D., KOTWICA, T., et al. Memristors: A short review on fundamentals, structures, materials and applications. *International Journal of Electronics and Telecommunications*, 2020, vol. 66, no. 2, p. 373–381. DOI: 10.24425/ijet.2020.131888

[9] HU, S. G., WU, S. Y., JIA, W. W., et al. Review of nanostructured resistive switching memristor and its applications. *Nanoscience and Nanotechnology Letters*, 2014, vol. 6, no. 9, p. 729–757. DOI: 10.1166/nnl.2014.1888

[10] MAZUMDER, P., KANG, S. M., WASER, R. Memristors: Devices, models, and applications. *Proceedings of the IEEE*, 2012, vol. 100, no. 6, p. 1911–1919. DOI: 10.1109/JPROC.2012.2190812

[11] SHIN, S., KIM, K., KANG, S. M. Memristor applications for programmable analog ICs. *IEEE Transactions on Nanotechnology,* 2011, vol. 10, no. 2, p. 266–274. DOI: 10.1109/TNANO.2009.2038610

[12] THOMAS, A. Memristor-based neural networks. *Journal of Physics D: Applied Physics,* 2013, vol. 46, no. 9, p. 1–12. DOI: 10.1088/0022-3727/46/9/093001

[13] PERSHIN, Y. V., DI VENTRA, M. Practical approach to programmable analog circuits with memristors. *IEEE Transactions on Circuits and Systems I: Regular Papers*, 2010, vol. 57, no. 8, p. 1857–1864. DOI: 10.1109/TCSI.2009.2038539

[14] WEY, T. A., JEMISON, W. D. Variable gain amplifier circuit using titanium dioxide memristors. *IET Circuits*, *Devices and Systems,* 2011, vol. 5, no. 1, p. 59–65. DOI: 10.1049/iet-cds.2010.0210

[15] YENER, S. C., MUTLU, R., KUNTMAN, H. A new memristor-based high-pass filter/amplifier: Its analytical and dynamical models. In *24th International Conference Radioelektronika.* Bratislava (Slovakia), 2014, p. 1–4. DOI: 10.1109/Radioelek.2014.6828420

[16] JOGLEKAR, Y. N., WOLF, S. J. The elusive memristor: Properties of basic electrical circuits. *European Journal of Physics*, 2009, vol. 30, no. 4, p. 661–675. DOI: 10.1088/0143-0807/30/4/001

[17] BIOLEK, Z., BIOLEK, D., BIOLKOVÁ, V. SPICE model of memristor with nonlinear dopant drift. *Radioengineering*, 2009, vol. 18, no. 2, p. 210–214. ISSN: 1805-9600

[18] PRODROMAKIS, T., PEH, B. P., PAPAVASSILIOU, C., et al. A versatile memristor model with nonlinear dopant kinetics. *IEEE Transactions on Electron Devices*, 2011, vol. 58, no. 9, p. 3099–3105. DOI: 10.1109/TED.2011.2158004

[19] ZHA, J., HUANG, H., LIU, Y. A novel window function for memristor model with application in programming analog circuits. *IEEE Transactions on Circuits and Systems II: Express Briefs*, 2016, vol. 63, no. 5, p. 423–427. DOI: 10.1109/TCSII.2015.2505959

[20] GALE, E. TiO_2-based memristors and ReRAM: Materials, mechanisms and models (a review). *Semiconductor Science and Technology*, 2014, vol. 29, no. 10, p. 1–10. DOI: 10.1088/0268-1242/29/10/104004

[21] BAGHEL, V. S., AKASHE, S. Low power memristor based 7T SRAM using MTCMOS technique. In *Fifth International Conference on Advanced Computing & Communication Technologies (ACCT)*. Haryana (India), 2015, p. 222–226. DOI: 10.1109/ACCT.2015.58

[22] GIBBONS, J. F., BEADLE, W. E. Switching properties of thin NiO films. *Solid-State Electronics*, 1964, vol. 7, no. 11, p. 785–790. DOI: 10.1016/0038-1101(64)90131-5

[23] YAO, J., SUN, Z., ZHONG, L., et al. Resistive switches and memories from silicon oxide. *Nano Letters*, 2010, vol. 10, no. 10, p. 4105–4110. DOI: 10.1021/nl102255r

[24] KWON, D. H., KIM, K. M., JANG, J. H., et al. Atomic structure of conducting nanofilaments in TiO_2 resistive switching memory. *Nature Nanotechnology*, 2010, vol. 5, no. 2, p. 148–153. DOI: 10.1038/nnano.2009.456

[25] YANG, J. J., PICKETT, M. D., LI, X., et al. Memristive switching mechanism for metal/oxide/metal nanodevices. *Nature Nanotechnology,* 2008, vol. 3, no. 7, p. 429–433. DOI: 10.1038/nnano.2008.160

[26] AKINAGA, H., SHIMA, H. Resistive Random Access Memory (ReRAM) based on metal oxides. *Proceedings of the IEEE*, 2010, vol. 98, no. 12, p. 2237–2251. DOI: 10.1109/JPROC.2010.2070830

[27] WASER, R., AONO, M. Nanoionics-based resistive switching memories. *Nature Materials*, 2007, vol. 6, no. 11, p. 833–840. DOI: 10.1038/nmat2023

[28] CHOI, B. J., JEONG, D. S., KIM, S. K., et al. Resistive switching mechanism of TiO_2 thin films grown by atomic-layer deposition. *Journal of Applied Physics*, 2005, vol. 98, no. 3, p. 1–10. DOI: 10.1063/1.2001146

[29] XIE, H., WANG, M., KURUNCZI, P., et al. Resistive switching properties of HfO_2-based ReRAM with implanted Si/Al ions. In *AIP Conference Proceedings,* 2012, vol. 1496, no. 1, p. 26–29. DOI: 10.1063/1.4766481

[30] ZHOU, P., SHEN, H., LI, J., et al. Resistance switching study of stoichiometric ZrO_2 films for non-volatile memory application. *Thin Solid Films*, 2010, vol. 518, no. 20, p. 5652–5655. DOI: 10.1016/j.tsf.2009.10.034

[31] LINN, E., ROSEZIN, R., KUGELER, C., et al. Complementary resistive switches for passive nanocrossbar memories. *Nature Materials*, 2010, vol. 9, no. 5, p. 403–406. DOI: 10.1038/nmat2748

[32] ROSEZIN, R., LINN, E., NIELEN, L., et al. Integrated complementary resistive switches for passive high-density nanocrossbar arrays. *Electron Device Letters*, 2011, vol. 32, no. 2, p. 191–193. DOI: 10.1109/LED.2010.2090127

[33] KARAKULAK, E., MUTLU, R., UÇAR, E. Sneak path current equivalent circuits and reading margin analysis of complementary resistive switches based 3D stacking crossbar memories. *Informacije MIDEM*, 2014, vol. 44, no. 3, p. 235–241.

[34] KARAKULAK, E., MUTLU, R., UÇAR, E. Reconstructive sensing circuit for complementary resistive switches-based crossbar memories. *Turkish Journal of Electrical Engineering & Computer Sciences,* 2016, vol. 24, no. 3, p. 1371–1383. DOI: 10.3906/elk-1309-71

[35] GAO, L., ALIBART, F., STRUKOV, D. B. Programmable CMOS/memristor threshold logic. *IEEE Transactions on Nanotechnology*, 2013, vol. 12, no. 2, p. 115–119. DOI: 10.1109/TNANO.2013.2241075

[36] JUNG, C. M., JO, K. H., LEE, E. S., et al. Zero-sleep-leakage flip-flop circuit with conditional-storing memristor retention latch. *IEEE Transactions on Nanotechnology*, 2012, vol. 11, no. 2, p. 360–366. DOI: 10.1109/TNANO.2011.2175943

[37] ROBINETT, W., PICKETT, M., BORGHETTI, J., et al. A memristor-based nonvolatile latch circuit. *Nanotechnology*, 2010, vol. 21, no. 23, p. 1–6. DOI: 10.1088/0957-4484/21/23/235203

[38] XIA, Q., ROBINETT, W., CUMBIE, M. W., et al. Memristor-CMOS hybrid integrated circuits for reconfigurable logic. *Nano Letters*, 2009, vol. 9, no. 10, p. 3640–3645. DOI: 10.1021/nl901874j

[39] EDWARDS, A. H., BARNABY, H. J., CAMPBELL, K. A., et al. Reconfigurable memristive device technologies. *Proceedings of the IEEE*, 2015, vol. 103, no. 7, p. 1004–1033. DOI: 10.1109/JPROC.2015.2441752

[40] JO, K. H., JUNG, C. M., MIN, K. S., et al. Self-adaptive write circuit for low-power and variation tolerant memristors. *IEEE Transactions on Nanotechnology,* 2010, vol. 9, no. 6, p. 675–678. DOI: 10.1109/TNANO.2010.2052108

[41] VOURKAS, I., SIRAKOULIS, G. C. Emerging memristor-based logic circuit design approaches: A review. *IEEE Circuits and Systems Magazine*, 2016, vol. 16, no. 3, p. 15–30. DOI: 10.1109/MCAS.2016.2583673

[42] WANG, F. Z., HELIAN, N., WU, S., et al. Delayed switching in memristors and memristive systems. *IEEE Electron Device Letters*, 2010, vol. 31, no. 7, p. 755–757. DOI: 10.1109/LED.2010.2049560

[43] XIE, Y. Modeling, architecture, and applications for emerging memory technologies. *IEEE Design & Test of Computers*, 2011, vol. 28, no. 1, p. 44–51. DOI: 10.1109/MDT.2011.20

[44] WANG, F. Z., HELIAN, N., WU, S., et al. Delayed switching applied to memristor neural networks. *Journal of Applied Physics*, 2012, vol. 111, no. 7, p. 1–3. DOI: 10.1063/1.3672409

[45] OZGUVENC, A., MUTLU, R., KARAKULAK, E. Sawtooth signal generator with a memristor. In *1st International Conference on Engineering Technology and Applied Sciences.* Afyon (Turkey), 2016, p. 1–6.

[46] YENER, S. C., MUTLU, R., YENER, T., et al. Memristor-based timing circuit. In *2017 Electric Electronics, Computer Science, Biomedical Engineerings' Meeting (EBBT'2017)*. Istanbul (Turkey), 2017, p. 1–3. DOI: 10.1109/EBBT.2017.7956776

[47] MUTLU, R., KARAKULAK, E. A methodology for memristance calculation. *Turkish Journal of Electrical Engineering & Computer Sciences*, 2014, vol. 22, no. 1, p. 121–131. DOI: 10.3906/elk-1205-16

[48] VONGEHR, S., MENG, X. The missing memristor has not been found. *Scientific Reports*, 2015, vol. 5, no. 1, p. 1–7. DOI: 10.1038/srep11657

[49] SONI, K., SAHOO, S. A review on different memristor modeling and applications. In *2022 International Mobile and Embedded Technology Conference (MECON).* Noida (India), 2022, p. 688–695. DOI: 10.1109/MECON53876.2022.9752214

[50] https://en.wikipedia.org/wiki/Zeno%27s_paradoxes

[51] CARRASCO-AGUILAR, M. A., MORALES-LÓPEZ, F. E., SÁNCHEZ-LÓPEZ, C., et al. Flux-charge analysis and experimental verification of a parallel memristor-capacitor circuit. *Memories-Materials, Devices, Circuits and Systems,* 2023, vol. 4, p. 1–6. DOI: 10.1016/j.memori.2023.100043

[52] PERSHIN, Y. V., DI VENTRA, M. A simple test for ideal memristors. *Journal of Physics D: Applied Physics*, 2018, vol. 52, no. 1, p. 1–4. DOI: 10.1088/1361-6463/aae680

[53] ADHIKARI, S. P., SAH, M. P., KIM, H., et al. Three fingerprints of memristor. *IEEE Transactions on Circuits and Systems I: Regular Papers*, 2013, vol. 60, no. 11, p. 3008–3021. DOI: 10.1109/TCSI.2013.2256171

[54] MUSTAFA, J., WASER, R. A novel reference scheme for reading passive resistive crossbar memories. *IEEE Transactions on Nanotechnology,* 2006, vol. 5, no. 6, p. 687–691. DOI: 10.1109/TNANO.2006.885016

[55] WITRISAL, K. Memristor-based stored-reference receiver–the UWB solution? *Electronics Letters*, 2009, vol. 45, no. 14, p. 713–714. DOI: 10.1049/el.2009.0123

[56] MASSOUD, Y., XIONG, F., SMAILI, S. A memristor-based random modulator for compressive sensing systems. In *2012 IEEE International Symposium on Circuits and Systems (ISCAS).* Seoul (South Korea), 2012, p. 2445–2448. DOI: 10.1109/ISCAS.2012.6271793

[57] GÖKNAR, I. C., ÖNCÜL, F., MINAYI, E. New memristor applications: AM, ASK, FSK, and BPSK modulators. *IEEE Antennas and Propagation Magazine*, 2013, vol. 55, no. 2, p. 304–313. DOI: 10.1109/MAP.2013.6529381

[58] ABUELMA'ATTI, M. T., KHALIFA, Z. J. A new memristor emulator and its application in digital modulation. *Analog Integrated Circuits and Signal Processing*, 2014, vol. 80, p. 577–584. DOI: 10.1007/s10470-014-0364-3

[59] WEY, T. A., BENDERLI, S. W. Amplitude modulator circuit featuring TiO_2 memristor with linear dopant drift. *Electronics Letters*, 2009, vol. 45, no. 22, p. 1103–1104. DOI: 10.1049/el.2009.2174

[60] TRUONG, S. N., VAN PHAM, K., YANG, W., et al. New pulse amplitude modulation for fine tuning of memristor synapses. *Microelectronics Journal*, 2016, vol. 55, p. 162–168. DOI: 10.1016/j.mejo.2016.07.010

[61] FOUDA, M. E., RADWAN, A. G. Power dissipation of memristor-based relaxation oscillators. *Radioengineering*, 2015, vol. 24, no. 4, p. 968–973. DOI: 10.13164/re.2015.0968

[62] DI VENTRA, M., PERSHIN, Y. V., CHUA, L. O. Circuit elements with memory: Memristors, memcapacitors, and meminductors. *Proceedings of the IEEE*, 2009, vol. 97, no. 10, p. 1717–1724. DOI: 10.1109/JPROC.2009.2021077

About the Authors …

Reşat MUTLU was born in Tekirdağ, Türkiye, in 1973. He received B.Sc. degree from YILDIZ Teknik University in Electrical Engineering in 1995 and M.Sc. and Ph.D. degrees from Rensselaer Polytechnic Institute in Electric Power Engineering in 1998 and 2004, respectively. He is currently an Associate Professor at the Department of Electronics and Telecommunication Engineering, Tekirdağ Namik Kemal University, Türkiye. His main research interests are modeling of memristor and memristive systems, analog and digital applications of memristive systems, analysis and modeling of resistive sintering systems.

Tuğçe Dabanoğlu KUMRU was born in Manisa, Türkiye, in 1992. She received her B.Sc. and M.Sc. degrees from Electronics and Telecommunication Engineering Department Tekirdağ Namik Kemal University, in 2015 and 2021, respectively. Her research interests include memristor and tractor systems.